Atmos. Chem. Phys., 12, 1995–2006, 2012
www.atmos-chem-phys.net/12/1995/2012/
doi:10.5194/acp-12-1995-2012

Atmospheric Chemistry and Physics

Evaluation of the smoke-injection height from wild-land fires using remote-sensing data

M. Sofiev[1], **T. Ermakova**[2], **and R. Vankevich**[2]

[1]Finnish Meteorological Institute, Finland
[2]Russian State Hydrometeorological University, Russia

Correspondence to: M. Sofiev (mikhail.sofiev@fmi.fi)

Received: 27 September 2011 – Published in Atmos. Chem. Phys. Discuss.: 17 October 2011
Revised: 24 January 2012 – Accepted: 9 February 2012 – Published: 21 February 2012

Abstract. A new methodology for the estimation of smoke-injection height from wild-land fires is proposed and evaluated. It is demonstrated that the approaches developed for estimating the plume rise from stacks, such as the formulas of G. Briggs, can be formally written in terms characterising the wild-land fires: fire energy, size and temperature. However, these semi-empirical methods still perform quite poorly because the physical processes controlling the uplift of the wildfire plumes differ from those controlling the plume rise from stacks. The proposed new methodology considers wildfire plumes in a way similar to Convective Available Potential Energy (CAPE) computations. The new formulations are applied to a dataset collected within the MISR Plume Height Project for about 2000 fire plumes in North America and Siberia. The estimates of the new method are compared with remote-sensing observations of the plume top by the MISR instrument, with two versions of the Briggs' plume-rise formulas, with the 1-D plume-rise model BUOYANT, and with the prescribed plume-top position (the approach widely used in dispersion modelling). The new method has performed significantly better than all these approaches. For two-thirds of the cases, its predictions deviated from the MISR observations by less than 500 m, which is the uncertainty of the observations themselves. It is shown that the fraction of "good" predictions is much higher (>80 %) for the plumes reaching the free troposphere.

1 Introduction

Biomass burning is one of the major contributors of trace gases and aerosols to the atmosphere, which significantly affects its chemical and physical properties. In addition to solid and gaseous material, fires release large amount of heat. The resulting buoyancy generates strong updrafts above the fire, which control the tracer distribution through rapid transport to the upper part of the atmospheric boundary layer (ABL) and the free troposphere (FT) (Freitas et al., 2007; Labonne et al., 2007), sometimes reaching the stratosphere (Fromm et al., 2000; Luderer et al., 2006).

Most of atmospheric composition models distribute the fire emissions homogeneously starting from the ground up to prescribed height H_p, which is sometimes region-dependent. For global chemistry-transport models, Davison (2004); Forster et al. (2001); and Liousse et al. (1996) set it to about 2 km, whereas Westphal and Toon (1991) used 5–8 km for regional simulations of smoke from intense Canadian fires. On the basis of observations from different field experiments, Lavoué et al. (2000) found a linear relationship between the plume height and the fire-line intensity with correlation coefficient of 0.95 and proportionality constant of 0.23 $m^2\,kW^{-1}$. They further showed that H_p is usually about 2–3 km for fires in the northern latitudes, but can reach 7–8 km for powerful crown fires. The biomass burning in Central America is usually less intense, therefore $H_p \sim 0.9$–1.5 km was suggested by Kaufman et al. (2003). Following this estimation, Wang et al. (2006) used 1.2 km (8th model layer) for the mesoscale simulations and conducted sensitivity studies showing 15 % variation of the near-surface concentrations if H_p is varied plus-minus one model layer (a few hundreds of meters).

Despite the apparent near-consensus among the modellers in using prescribed fire injection height, H_p is strongly dependent on meteorological conditions and fire intensity, which are both highly dynamic. In particular, favourable meteorological conditions are necessary for the smoke to reach the stratosphere (Labonne et al., 2007; Luderer et al., 2006; Trentmann et al., 2006).

Recently, remote-sensing observations of the plume heights became available from the Multi-angle Imaging SpectroRadiometer (MISR) instrument onboard NASA Terra satellite (Mazzoni et al., 2007; http://www-misr.jpl.nasa.gov). Using the database of the MISR Plume Height Project, Sofiev et al. (2009) showed that more than 80 % of the fires observed in 2007–2008 over the US injected their smoke within the ABL. This estimate was supported by the extensive analysis of Val Martin et al. (2010).

One of the widely-known approaches to dynamic evaluation of the injection height was developed by Freitas et al. (2007), who embedded a 1-D plume-rise model into a 3-D atmospheric dispersion model and demonstrated the importance of the water-condensation heat for plume-rise estimations. The module was included into WRF-Chem model and used in studies related to biomass burning (Pfister et al., 2011). However, the system requires integration of a set of 1-D differential equations for each fire, which may be expensive for large-scale applications. Also, Pfister et al. (2011) pointed out that about 50 % of the fire emissions were attributed to the free troposphere, which is in apparent contradiction with the MISR set statistics, where only ∼15 % of the plumes reach FT.

A specific problem of the fire plumes is that the characteristics of this type of source differ from the parameters considered by the existing plume-rise formulations and models. In particular, all such approaches require the diameter of the buoyant plume at the stack top (considered to have circular cross-section), temperature and velocity of the outgoing gases, their density, etc. (Briggs, 1984; Freitas et al., 2007; Nikmo et al., 1999; Weil, 1988). These quantities are hard to define for wild-land fires, which have strongly non-circular shape (rather a bow- or kidney-shape), wide overheated surface area with strongly-varying temperature in different parts of the burning area, no stack or definite release height, and strongly-varying initial velocity of fumes in different parts of the fire. Therefore, the necessity of the development of an approach adapted to the specifics of the wild-land fires is evident.

The objective of the current study is to develop and evaluate an approach for computing the plume injection height for wild-land fires and to compare its performance with the existing approaches. The method is developed for usage within 3-D chemistry transport models.

The paper is organised as follows. The next section summarises the existing plume-rise formulations used for the comparison. Section 3 outlines the datasets used by this study for the development. The new algorithm is derived in Sect. 4. Section 5 presents the comparison of the new methodology with the existing approaches. Finally, Sect. 6 considers peculiarities of the new formulations.

2 Existing plume-rise formulations

The most widely known formulations of the plume height from buoyant sources belong to G. Briggs. In the middle of the twentieth century he compared nine formulas of this type using data from sixteen different sources and concluded that the best fit to the data was obtained using the "2/3 law" with a certain termination distance. The 2/3 law states that plume rise is directly proportional to the power 2/3 of the downwind distance from the source x^*. Originally, it was formulated in the following form (Briggs, 1969; Guldberg, 1975):

$$H_{\mathrm{C}} = \begin{bmatrix} 1.6F^{1/3}(3.5x^*)^{2/3}U^{-1} \\ 2.4(F/Us)^{1/3} \\ 5F^{1/4}s^{-3/8} \end{bmatrix} = \begin{bmatrix} \begin{bmatrix} 21.4F^{3/4}U^{-1}, & F < 55\,\mathrm{m^4\,s^{-3}} \\ 38.7F^{3/5}U^{-1}, & F \geq 55\,\mathrm{m^4\,s^{-3}} \end{bmatrix} & \text{neutral, unstable} \\ 2.4(F/Us)^{1/3}, & \text{stable,} \quad U > 0.5\,\mathrm{m\,s^{-1}}, \\ 5F^{1/4}s^{-3/8}, & \text{stable,} \quad U \leq 0.5\,\mathrm{m\,s^{-1}} \end{bmatrix} \quad (1)$$

where H_{C} is final rise of the plume centerline from the stack top, $F = g v_{\mathrm{s}} r^2 (1 - \rho_{\mathrm{p}}/\rho_{\mathrm{a}})$ is buoyancy flux parameter, g is acceleration due to gravity, v_{s} is stack gas exit velocity, r is stack exit radius, ρ_{a} is ambient air density, ρ_{p} is plume density, x^* is distance at which the atmospheric turbulence begins to dominate over the entrainment, U is mean horizontal wind speed averaged from the top of the stack to the top of the plume, $s = \frac{g}{T_{\mathrm{a}}} \frac{\partial \theta}{\partial z}$ is buoyancy parameter, θ is potential air temperature, T_{a} is absolute air temperature. Hereinafter, equation-set (1) is referred to as B69.

Numerous subsequent refinements were mainly aiming at a better reflection of the details of meteorological conditions and, to some extent, more detailed source description. By the mid-80s, a set of more sophisticated formulations had emerged (Briggs, 1984; Weil, 1988):

$$H_{\mathrm{C}} = \begin{bmatrix} 2.1\left(\frac{r v_{\mathrm{s}}^3}{N^2 \Phi^2 U}\right)^{1/3}, & \text{stable} \\ 0.76\left(\frac{r v_{\mathrm{s}}^3}{u_*^2 \Phi^2 U}\right), & \text{neutral} \\ 4.5\left(\frac{r v_{\mathrm{s}}^3 z_i^{2/3}}{4 w_*^2 \Phi^2 U}\right)^{3/5}, & \text{unstable} \end{bmatrix} \quad (2)$$

Here N is the Brunt-Väisälä frequency, u_* is the friction velocity, w_* is the convection scale velocity, z_i is the height of the nearest inversion layer above the stack top, $\Phi = v_{\mathrm{s}}/\sqrt{gr(1-\rho_{\mathrm{p}}/\rho_{\mathrm{a}})}$ is the Froude number. This version is further referred to as B84.

These and other formulations (e.g. Berlyand, 1975, Fire Emission Production Simulator (FEPS), VSMOKE, Lavdas, 1996) have a common weak point: they assume a vertically-homogeneous atmosphere, which can be described via some parameters taken (in practice) at the top of the stack. This can be acceptable only if both the stack top and the plume injection height are within the ABL or both are in the FT. The assumption is evidently wrong if the stack is inside the ABL whereas the plume buoyancy is sufficient to reach the FT. More discussion and a list of limitations can be found in Briggs (1984).

A more sophisticated approach is taken by the 1-D plume-rise models, such as the BUOYANT (Martin et al., 1997), BUO-FMI (Nikmo et al., 1999), FIREPLUME (Brown et al., 1997; Brown, 1997), model of Freitas et al. (2007), DAYSMOKE (Liu et al., 2010), and others. These systems still assume the horizontal symmetry of the plume and use the formulations integrated across it. However, they explicitly integrate a system of 1-D equations for energy, mass, and momentum of the buoyant plume along the trajectory of the plume centreline. The centreline position and the plume width are computed as functions of time and/or horizontal distance from the source point. This approach allows for direct consideration of the vertical structure of the atmosphere, which is usually simplified by considering only two layers – ABL and FT – with prescribed temperature and wind speed gradients in each of them. An additional peculiarity of the FIREPLUME model is that it considers the latent heat and phase transition of water vapour, which can significantly increase the plume rise.

3 Input data for plume-rise computations

The input information needed for any plume-rise approach consists of the data describing the buoyant source and the meteorological conditions at the place of the fire.

For the current study, the information on the wild-land fires is obtained from the active-fire observations by MODIS instrument onboard Aqua and Terra satellites (http://modis.gsfc.nasa.gov). The MODIS collection 5 of the active fire characteristics includes the following parameters: (i) radiative temperatures of the overheated pixel and the surrounding background pixels; (ii) emission rate of the radiative energy from the pixel, the Fire Radiative Power (FRP, [W]). The inter-relations of these parameters were considered by Sofiev et al. (2009). This dataset is essentially the only existing collection that covers the whole globe over more than a decade (the Terra satellite was launched in 2000, Aqua in 2002) and observes the actual on-going fires rather than the burnt area.

The only source of meteorological information which would cover the whole globe and could be co-located with the fire observations, is atmospheric modelling by a global Numerical Weather Prediction (NWP) system. For the current study, we used the operational archives of the European Centre for Medium-Range Weather Forecast (ECMWF). We involved the dry-parcel method of the ABL height estimation after Sofiev et al. (2006).

The observations of the injection height were taken from the database of the MISR Plume Height Project (Kahn et al., 2008; Mazzoni et al., 2007). For the current study we used all information available by its start, which included injection heights for about 2000 fires that took place in the US, Canada, and Siberia during 2007–2008 fire seasons. These datasets were arbitrarily split into "learning" and "control" subsets in proportion 70–30 %.

Importantly, MISR is onboard the satellite Terra together with one of the MODIS devices, which provides a perfect co-location in space and time between the active-fire observations by MODIS and the fire plume heights measurements by MISR.

4 Methodology for injection height estimation adapted to wild-land fires

We shall derive a general form of the dependence of injection height on fire characteristics and meteorological conditions using strongly-simplified analytical considerations. The obtained relations will be then turned into a function with several empirical constants, which will be found from fitting to the MISR observations.

An analytical function describing the plume rise from a wild-land fire can be obtained by assuming that the heat energy of the fire is spent only against buoyancy forces. Such an approach changes the criterion for the end of the rise: the plume comes to equilibrium with the surrounding air when the energy excess pumped into it by the fire is fully spent in the uplift. This approach has common features with the CAPE (Convective Available Potential Energy) formulations used for describing deep convection and thunderstorms (see Moncrieff and Miller, 1976 and p. 80–81 of Barry and Chorley, 1998). Importantly, it is totally different from the criterion for the stack plume-rise where the wind-induced bending is the key factor.

For qualitative analysis of the dependencies let us consider only two processes: the uplift against the atmospheric stratification and the plume widening due to entrainment of the surrounding air.

Let the fire energy E_0 be pumped into an air volume V while it is in contact with the flames. Then the density of the energy excess e_0 in comparison with the undisturbed surrounding air will be:

$$e_0 = \frac{E_0}{V} = \frac{E_0}{S_\mathrm{f} w \tau} = \frac{P_\mathrm{f}}{S_\mathrm{f} w} \tag{3}$$

Here w is the initial mean vertical velocity of the plume, τ is the time period during which the volume is in contact with flames, S_f is the fire area (of any shape), and P_f is the fire power released into the air.

The initial energy excess can be expressed in terms of difference of initial temperatures of the plume T_p^0 and ambient air T_a^0: $e_0 = c_p \rho_\mathrm{a} (T_\mathrm{p}^0 - T_\mathrm{a}^0)$, where c_p is specific heat capacity at constant pressure of air, ρ_a is air density. If the plume rises adiabatically, then $\frac{\mathrm{d}(T_\mathrm{p} - T_\mathrm{a})}{\mathrm{d}z} = -\frac{\mathrm{d}\theta}{\mathrm{d}z}$ (θ is potential temperature of the ambient air) and the change of the energy excess $e(z)$ during the uplift can be written as:

$$\frac{\mathrm{d}e}{\mathrm{d}z} = -c_p \rho_\mathrm{a} \frac{\mathrm{d}\theta}{\mathrm{d}z} - \frac{E_0}{V^2} \frac{\mathrm{d}V}{\mathrm{d}z} \tag{4}$$

The first term characterizes the change of the temperature difference between the plume and ambient air, whereas the second term reflects plume widening. Assuming constant cross-plume horizontal diffusivity $K_{\rm hor}$ and constant speed of the uplift w, one obtains linear growth of the plume cross-section area S with height (see sections 18.4–18.6 and p. 845 of Seinfeld and Pandis, 2006):

$$\frac{{\rm d}\sigma^2}{{\rm d}z} = \frac{2K_{\rm hor}}{w}\,, \quad \Rightarrow \quad S = \pi r^2 \sim 3\pi\sigma^2 = \frac{6\pi K_{\rm hor}}{w} z + S_{\rm f} \qquad (5)$$

Here r is fire radius and $S_{\rm f}$ is fire area. Introducing Brunt-Väisälä frequency N instead of ${\rm d}\theta/{\rm d}z$ and noticing that for constant w, ${\rm d}V/{\rm d}z = w\tau\,{\rm d}S/{\rm d}z$, one can write Eq. (4) as:

$$\frac{{\rm d}e}{{\rm d}z} = -\frac{c_p\rho_{\rm a}\theta}{g}N^2 - \frac{6\pi K_{\rm hor}}{w^2(S_{\rm f}+6\pi z K_{\rm hor}/w)^2}P_{\rm f} \qquad (6)$$

This equation should be integrated with the boundary condition $e(0) = e_0$. The final height of the plume top $H_{\rm p}$ is then determined via $e(H_{\rm p}) = 0$.

If all parameters in Eq. (6) are assumed to be constant, the change of the variables from height $z$to normalised plume cross-section area $\xi = S/S_{\rm f}$ followed by integration renders quadratic equation for $\xi_{\rm p}(z = H_{\rm p})$:

$$-\frac{c_p\rho_{\rm a}\theta S_{\rm f}^2 w N^2}{6\pi g K_{\rm hor}}\xi_{\rm p}^2 + \frac{P_{\rm f}}{w}\xi_{\rm p} + \frac{P_{\rm f}}{w} = 0$$
$$\xi_{\rm p} = 1 + \frac{6\pi H_{\rm p} K_{\rm hor}}{S_{\rm f} w} \qquad (7)$$

Its solution is:

$$\xi_{\rm p} = \frac{P_{\rm f}}{AN^2}\left(1 + \sqrt{1 + \frac{2AN^2}{P_{\rm f}}}\right), \quad A = \frac{c_p\rho_{\rm a}\theta w^2 S_{\rm f}^2}{3\pi g K_{\rm hor}} \qquad (8)$$

This solution (Eq. 8) can be turned into a generic formula for $H_{\rm p} = f(P_{\rm f}, N, ...)$ with a few unknown constants to be determined empirically.

Firstly, the variable A has to be taken as a normalising constant. It incorporates poorly-known parameters, which cannot be evaluated with the information available in real-life cases. Its value can be roughly estimated taking $S_{\rm f} \sim 10^3\,{\rm m}^2$, $w \sim 1\,{\rm m\,s}^{-1}$, $K_{\rm hor} \sim 1\,{\rm m}^2\,{\rm s}^{-1}$. Then $A \sim 4\times10^9$ Js. This normalization can formally be written as a ratio of reference fire power $P_{\rm f0}$ and Brunt -Väisälä frequency N_0:

$$A = \frac{P_{\rm f0}}{N_0^2}\,, \quad P_{\rm f0} = 10^6\,{\rm W}\,, \quad N_0^2 = 2.5\times10^{-4}\,{\rm s}^{-2} \qquad (9)$$

Secondly, the fire energy $P_{\rm f}$ spent on the air heating and the FRP observed from space are linearly related to the consumed biomass and close to each other (Kaufman et al., 1998; Sukhinin et al., 2005), thus allowing us to assume that $P_{\rm f}$ FRP.

Thirdly, for typical values of atmospheric and fire parameters, AN^2/FRP varies from 1 to 100. From the corresponding asymptote of the solution (Eq. 8), one can see that the injection height will be proportional to FRP to the power of 0.5. This, however, is the upper limit of $H_{\rm p}$ because additional losses to friction and changing atmospheric and plume parameters (e.g. gradual slowing down of the rise and faster-than-linear widening of the plume with height) will result in a smaller power $\gamma < 0.5$.

Fourthly, Brunt-Väisälä frequency is an external parameter with regard to fire and varies strongly with altitude. Therefore, the ratio $P_{\rm f}/N^2$ in Eq. (8) cannot be expected to stay as a unique descriptor of the case. We shall consider these variables separately. To avoid problems with $N^2 \le 0$ inside the unstable ABL, we shall take its FT value $N = N_{\rm ft}(z \approx 2H_{\rm abl})$ but allow for some part of the ABL passed "freely" by adding a fraction of $H_{\rm abl}$ to $H_{\rm p}$. In addition, instead of N_0^2/N^2 we shall use $\exp(-N^2/N_0^2)$, which for small N^2 limits the $H_{\rm p}$ growth by replacing N_0^2/N^2 with $1/(1+N^2/N_0^2)$. For large N^2 it quickly approaches zero, as one would expect for very stable stratification.

Finally, introducing the empirical calibration constants, we obtain the generic formula:

$$H_{\rm p} = \alpha H_{\rm abl} + \beta\left(\frac{\rm FRP}{P_{\rm f0}}\right)^{\gamma}\exp\left(-\delta N_{\rm FT}^2/N_0^2\right) \qquad (10)$$

Here the constants are: α is the part of ABL passed freely, β weights the contribution of the fire intensity, γ determines the power-law dependence on FRP, δ defines the dependence on stability in the FT. Their ranges follow from the above considerations:

$$\alpha < 1\,; \quad \beta > 0\,{\rm m}\,; \quad \gamma < 0.5\,; \quad \delta \ge 0 \qquad (11)$$

4.1 Identification and evaluation of parameters of Eq. (10)

Identification of the constants in the Eq. (10) was based on the learning sub-set of the MISR fire observations (70 % of the MISR collection, 1278 fires).

Since both FRP and $H_{\rm p}$ observations have a noticeable fraction of outliers, utilization of the standard L_2 (least-squares) fitting criterion is not advisable (Huber, 1981). Instead, the ranking sum $J_{\rm R}$ was used:

$$J_{\rm R} = \sum_{i=1}^{N_{\rm fires}}\Theta\left(\left|H_{\rm p}^{\rm obs}(i) - H_{\rm p}^{\rm mdl}(i)\right| - \Delta h\right),$$
$$\Theta(x) = \begin{cases} 0\,, & x \le 0 \\ 1\,, & x > 0 \end{cases} \qquad (12)$$

Here Δh is the desired accuracy of the prediction, [m], $N_{\rm fires}$ is the number of fires in the subset, $H_{\rm p}^{\rm obs}(i)$ and $H_{\rm p}^{\rm mdl}(i)$ are the observed and predicted plume top heights of the i-th fire.

Following Kahn et al. (2007), the MISR actual accuracy was taken to be 500 m, which was used as the Δh value. As a result, only the predictions indistinguishable from the

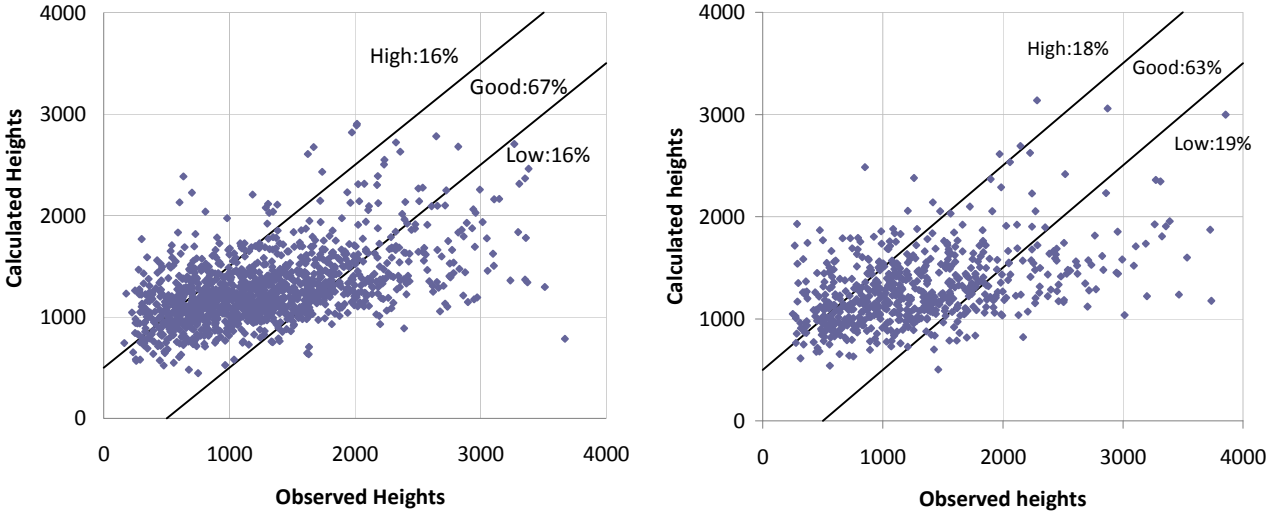

(a) Learning subset, Eqs. (10, 13)

(b) Control subset, Eqs. (10, 13)

Fig. 1. Comparison of predictions of the formula (10) with the observed H_p for the learning (panel **a**) and control (panel **b**) subsets. Parameter values (Eq. 13). Unit = [m].

MISR estimates were considered as "good" by the cost function (Eq. 12), whereas those falling outside the MISR uncertainty range were penalised.

The fitting gave the following parameters:

$$\alpha = 0.24\,; \quad \beta = 170\,\mathrm{m}\,; \quad \gamma = 0.35\,; \quad \delta = 0.6 \tag{13}$$

The quality of the fit is demonstrated in Fig. 1a, which shows that the formula (10) with the parameters (Eq. 13) predicts about two thirds of the learning-set cases within 500 m of the MISR observations. These values are for the whole learning subset but the difference between the North American and Siberian cases did not exceed 5 %.

The formulation (Eqs. 10, 13) was evaluated using the control MISR subset (Fig. 1b). Comparing the scatterplots in panels (a) and (b), one can see that the performance of the suggested procedure over the control dataset is essentially the same as that over the learning subset. The scores for the American and Siberian control-set fires differ by less than 10 % (not shown). The heights of the top of the plumes predicted with this method are within uncertainty of the MISR observations in two-thirds of the cases for both locations.

For the above calculations, we used all available MISR observations without filtering out the data with "fair" or "poor" confidence. If one takes only "good" cases, the scores grow by about 10 % (>70 % of the predictions appear within 500 m of the observations) but the datasets become three times smaller, thus raising doubts about statistical significance and stability of the obtained coefficients.

5 Comparison with other approaches

In this section, we compare the four approaches (B69, B84, BUOYANT model, and the new formula 10) using the whole MISR dataset (1913 fires). The comparison required two pre-processing steps: (i) extra characteristics of the fires and meteorological variables were calculated to satisfy the input requirements of BUOYANT; (ii) B69 and B84 formulas were rewritten using the variables available from MODIS and MISR.

5.1 Extra parameters describing wildfire

MODIS observations of temperature and FRP of the burning pixel at several wavelengths enable estimation of the area of the fire S_f and its radiative temperature T_f. Following Dozier (1981), let us consider the burning pixel seen by the satellite with radiative temperature T_{rad} as a combination of two parts: the fire and the undisturbed background with areas S_f and S_b, and temperatures T_f and T_b, respectively. These two sub-areas emit radiative energy recorded by the satellite at two frequencies ν_1 and ν_2. Using Planck's law, one can write:

$$\frac{2h\nu_i^3(S_f+S_b)}{c^2(\exp(h\nu_i/kT_{rad}))} = \frac{2h\nu_i^3 S_f}{c^2(\exp(h\nu_i/kT_f))} + \frac{2h\nu_i^3 S_b}{c^2(\exp(h\nu_i/kT_b))}\,, \quad i = 1,2 \tag{14}$$

The system (Eq. 14) contains two equations for two frequencies and two unknowns: the ratio S_f/S_b and T_f. They were solved using standard products MOD14 of MODIS instrument (channels 21 and 31, which correspond to wavelengths

of ∼4 and ∼11 µm). The total pixel area $S_f + S_b$ is determined from the MODIS frame geometry, and the background environment temperature T_b is found from the neighbouring pixels. The system has to be solved numerically, resulting in fire radiative temperature T_f and its area S_f. Due to noise in the data, the solution does not always converge or may lead to unpredictable results if $T_f \sim T_b$ (in the later case, however, the pixel is usually not reported as an active fire). Such cases (a few % of the total dataset) were filtered out.

5.2 Adaptation of B69 and B84 for wild-land fires

In the equations B69 and B84, the buoyancy flux F (see Eq. 1 and notations there) has to be expressed in energy and temperature terms to make them applicable to MISR dataset. Applying the gas-state equation and taking into account that the plume molar mass is close to that of air, we obtain:

$$F = g v_s r^2 \frac{1/T_a - 1/T_p}{1/T_a} = \frac{g}{T_p} v_s r^2 (T_p - T_a)$$
$$= \frac{g}{\pi T_p} \frac{P_f}{c_p \rho_a} = \frac{g}{\pi T_p} \frac{\mathrm{FRP}}{c_p \rho_a} \quad (15)$$

The plume temperature T_p is the analogy to the stack-top temperature but, since there is no "top" of the wildfire, its exact definition is not possible. The actual temperature of outgoing gases varies from 700–1000 K (Lim et al., 2001) down to 350–400 K within short distance along the vertical (Gostintsev et al., 1991). Fortunately, T_p almost always (except for B84 neutral case) is taken to the power of 0.25–0.5, which reduces the impact of its uncertainty. As a rough estimation, we linked it to the fire radiative temperature T_f obtained from (Eq. 14):

$$T_p = T_a + \mathrm{const}\,(T_f - T_a) \quad (16)$$

The value const = 0.1 was selected to obtain the best estimates of B69 and B84 for the learning MISR dataset.

Since both B69 and B84 predict the centerline height H_C, conversion to the plume top height H_p has to be made. Following Briggs (1975), the plume thickness is taken equal to H_C, hence $H_p = 1.5 H_C$.

Taking into account that for fires $\mathrm{FRP}/T_p > 55\,\mathrm{m^4\,s^{-1}}$ almost always, for B69 we obtain:

$$H_p = \begin{cases} 5.7\left(\frac{g\,\mathrm{FRP}}{N^3 T_p c_p \rho}\right)^{1/4}, & \text{stable},\ U \le 0.5\,\mathrm{m\,s^{-1}} \\ 2.4\left(\frac{g\,\mathrm{FRP}}{N^2 U T_p c_p \rho}\right)^{1/3}, & \text{stable},\ U > 0.5\,\mathrm{m\,s^{-1}} \\ 29\left(\frac{g\,\mathrm{FRP}}{T_p c_p \rho}\right)^{3/5} U^{-1};, & \text{neutral, unstable} \end{cases} \quad (17)$$

The B84 equations will read:

$$H_p = \begin{cases} 2.7\left(\frac{g\,\mathrm{FRP}}{N^2 U c_p \rho T_p}\right)^{1/3}, & \text{stable} \\ 0.72\left(\frac{g\,\mathrm{FRP}}{u_*^2 U c_p \rho T_p}\right), & \text{neutral} \\ 1.1\left(\frac{g\,\mathrm{FRP} H_{ABL}^{2/3}}{w_*^2 U c_p \rho T_p}\right)^{3/5}, & \text{unstable} \end{cases} \quad (18)$$

5.3 Inter-comparison results

The scatterplots for all approaches applied to the whole MISR dataset are presented in Fig. 2 and the corresponding statistics are summarised in Table 1. Table 1 also includes the statistics for the persistency approach, which appoints the same value to all fires: 1289 m, the mean height of the learning MISR set. As one can see, the suggested formula performs better than any other approach and much better than other semi-empirical formulas. Comparable quality was demonstrated only by the BUOYANT model, which was directly solving the 1-D budget equations along the plume trajectory. Intriguingly, B69 and B84 scored even worse than the persistency method, which attributed one height (1289 m, mean over learning subset) to all fires. From one side, better performance of the persistency method than the Briggs' formulations provides certain justification for the prescribed plume distribution accepted by many atmospheric models. From another side, it raises questions about the reasons for the failure of the well-recognised methods in applications to wild-land fires.

The root-cause of the low scores of B69 and B84 is that they are based on numerous simplifications and empirical coefficients, which were selected for stacks rather than for wildfires. The poor quality of predictions originates from the inadequacy of these assumptions and, in particular, the wrong sets of governing parameters. For example, our analysis showed that the wind speed is unimportant for the wildfire plume height, in particular, the error of the formula (10) is not correlated with wind speed taken at any height (not shown). Conversely, it is the primary parameter for all approaches related to stacks. Admittedly, this conclusion is non-orthodox in comparison with generally accepted strong dependence of the injection height on wind. Certain insight into the problem can be found in the recent study of Freitas et al. (2010), who, based on model simulations, concluded that the ambient air entrainment due to wind shear can affect the injection height of small-size fire plumes. For wide-area plumes it had no impact. Assuming that this explanation holds in the current study, we are forced to conclude that the accuracy of the MISR plume top data and/or quality of the modelled wind speed are insufficient to detect the variations in the injection height of the small-size fires. This variability only adds to the scatter of the low plumes in the scatterplot of Fig. 2.

From Fig. 2, one can also notice a tendency towards underestimation of the BUOYANT model, which did not allow any single plume to rise above 3000 m. This is probably due to the missing latent heat contribution, which, according to Freitas et al. (2007), can substantially increase the injection height. The new approach is much less affected by this caveat: the effects of both sensible and latent heat are automatically taken into account during the calibration step. Since the latent heat release is not captured by the satellites as part of FRP, the calibration implicitly relies on limited

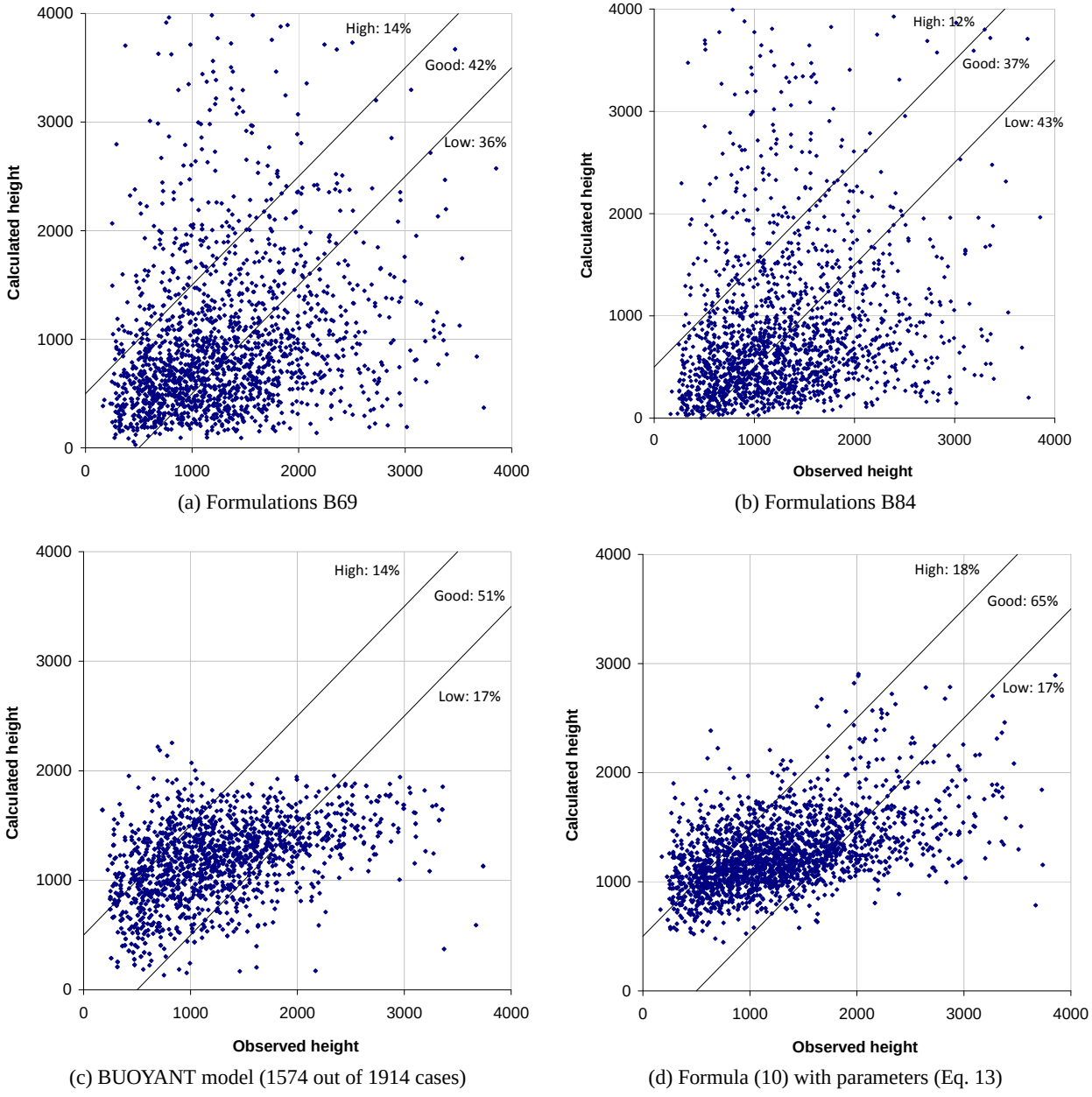

(a) Formulations B69

(b) Formulations B84

(c) BUOYANT model (1574 out of 1914 cases)

(d) Formula (10) with parameters (Eq. 13)

Fig. 2. Comparison of B69 (Eq. 17), B84 (Eq. 18), BUOYANT, and formula (10, 13) for the whole MISR set.

variability of the latent and sensible heat ratios to FRP. Violation of this assumption is probably one of the main contributors to the scatter of the model-measurement comparison.

6 Discussion

Comparison of the relative importance of the atmospheric and fire characteristics in Eq. (13) makes it evident that the success of the prediction strongly depends on quality of the modelled boundary-layer height and on the FRP observations. The Brunt-Väisälä frequency contributes only marginally: in most cases $\left|\delta N^2 / N_0^2\right| < 0.1$. One can expect, however, that the FT stability is partly reflected by the boundary-layer height (Zilitinkevich et al., 2007).

The added value of the combination of H_{ABL} and FRP is demonstrated in Fig. 3, which presents scatterplots of the observed injection height with regard to these parameters taken independently. As one can see, neither deep H_{ABL} nor high FRP taken separately can explain the injection height of the plume. This tendency was also noticed by Labonne et al. (2007); Luderer et al. (2006); Trentmann et al. (2006) for stratosphere-reaching plumes: it is the combination of favourable meteorological conditions and strong fire that results in high plumes.

Table 1. Performance of B69, B84, BUOYANT and formula (10) approaches for the MISR dataset.

	B69	B84	BUOYANT	Persistence	Formula (10)
Prediction within observational accuracy, %	42	37	51	55	65
Low predictions, %	36	43	17	21	17
High predictions, %	14	12	14	24	18
Failed analysis, %	8	8	18	–	–
Correlation coefficient	0.15	0.03	0.44	0	0.45
Range representation	2.6	8.0	0.54	0	0.48
RMSE [m]	1764	5555	604	716	646

Parameters:
Prediction within observational accuracy: a fraction (in %) of the predicted plume top heights deviating from the MISR observation by less than the MISR uncertainty of 500 m
Low prediction: fraction (in %) of the predicted plume top heights lower than the MISR observation by more than 500 m
High prediction: fraction (in %) of the predicted plume-top heights higher than the MISR observation by more than 500 m
Failed analysis: fraction (in %) of cases where computations have not converged
Correlation coefficient: Pearson's sample correlation coefficient taken over the MISR dataset
Range representation: a ratio of the observed and predicted sample standard deviations of the heights: $\sigma_{\mathrm{mdl}}/\sigma_{\mathrm{obs}}$
RMSE: root-mean-square error of the predicted heights, [m]
Note: large fraction of failed cases by BUOYANT is related to the model applicability range (computations failed for too low surface pressure in mountains, too high wind speed, too high T_{f}, etc).

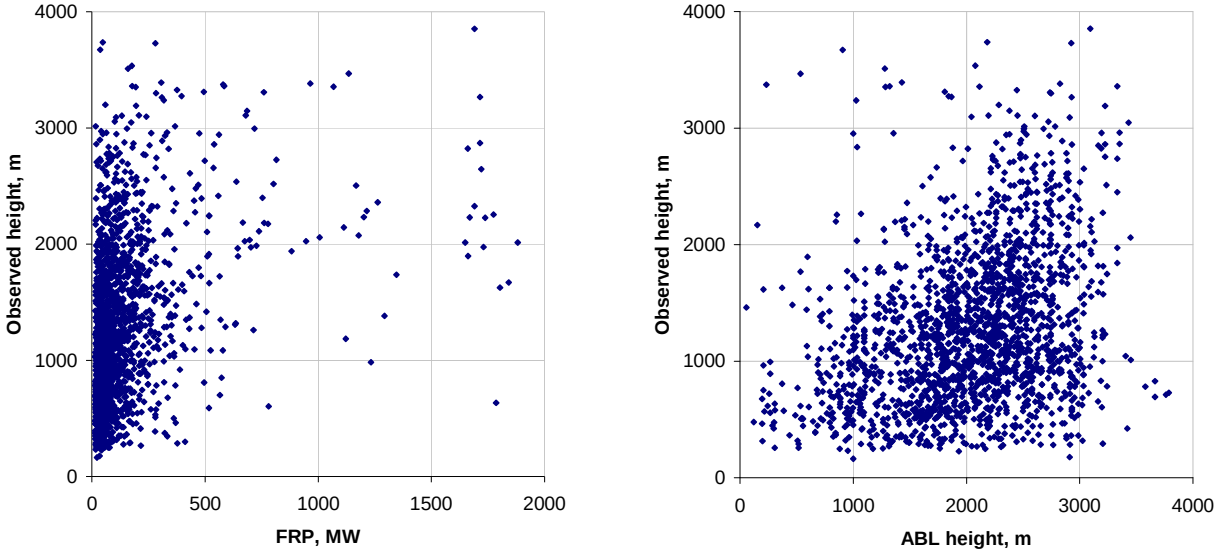

Fig. 3. Correlation of the observed plume height and individual components of the formula (10, 13): boundary layer height and FRP.

6.1 Prediction of free-troposphere plumes

The scatterplots for the suggested formula (Figs. 1 and 2d) make it evident that the predictions have noticeably lower dynamic range than the MISR observations (quantified in Table 1). That is, the new formula tends to over-estimate the low plumes and under-estimates the high ones. There was no easy way found to improve the range representation: correlation of the error with the basic atmospheric parameters (wind, temperature, stability, ABL height) is essentially zero.

One can argue that the plume height inside the boundary layer is quite an uncertain parameter and it is less important to predict it accurately in comparison with the plumes reach the FT. Indeed, intensive turbulent mixing quickly distributes the smoke over the whole ABL, thus making the question about the plume height rather academic. Prediction of the FT plumes seems to be more important since the vertical profiles of the smoke concentration would survive longer under stable stratification.

To investigate the possibility of predicting the height of the FT plumes with accuracy higher than that of Table 1, they were selected from the MISR learning subset (204 cases). The fitting procedure was then repeated only for these fires resulting in the following parameter values:

$$\alpha = 0.93; \quad \beta = 298\,\mathrm{m}; \quad \gamma = 0.13; \quad \delta = 0.7 \qquad (19)$$

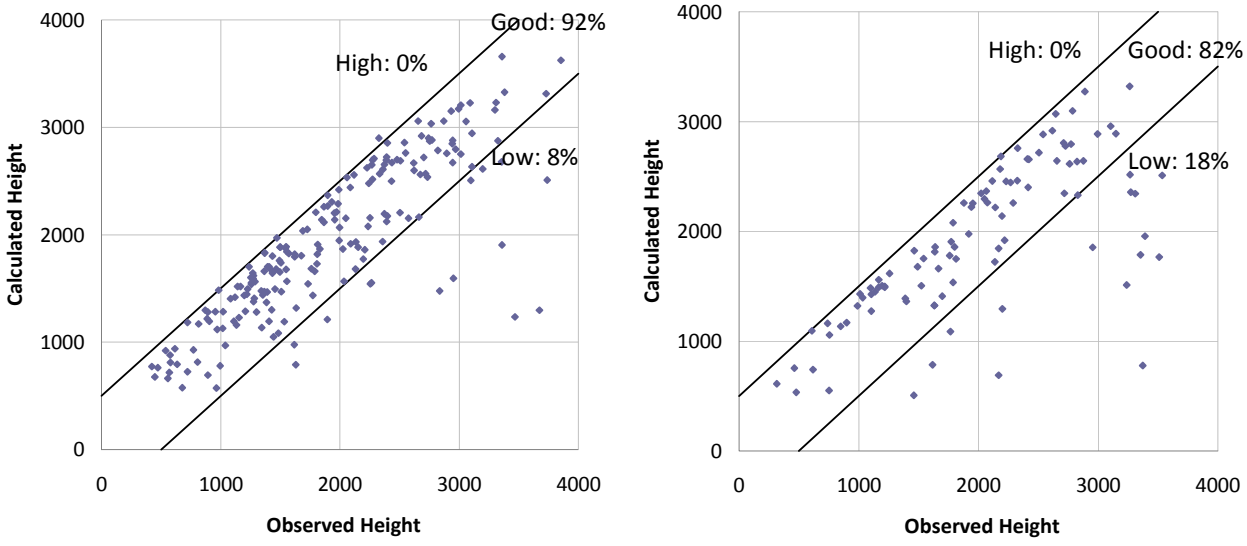

(a) Learning dataset (b) Control dataset

Fig. 4. Performance of the algorithm (Eq. 10, 19) for the free-troposphere plumes extracted from the learning (panels **a**) and control (panels **b**) MISR datasets. Unit = [m].

They are substantially different from (Eq. 13). In particular, the ABL is always passed "almost for free", whereas the FRP power γ has been reduced down to 1/5 reflecting the necessity of the plume to rise against the FT stable stratification. An attempt to refit the ABL-only fires does not lead to significant changes in the optimal coefficient values (Eq. 13).

The performance of fit (Eq. 19) for the FT cases from both learning and control sets is comparatively similar and outstandingly good: 92 and 82 % of the fires appear within 500 m of the observations (Fig. 4) for the learning and the control set, respectively. The 10 % difference in the scores is probably due to limited size of the sets.

There is, however, one peculiarity: in Fig. 4 the fit (Eq. 16) was applied to the plumes, which were known to reach FT: this information came from the MISR observations. In general case such information is not available, which raises the problem of identifying the above-ABL plumes. A seemingly evident solution, to compute H_p with the generic fit (Eq. 13) and then compare it to H_{ABL}, unfortunately leads to an unequivocal outcome. From one side, the scatterplot of Fig. 5 demonstrates that the method performs comparatively well: the bulk of the cases are correctly recognised to be inside ABL or to reach FT. But since the fraction of the FT plumes is barely 15 % and the fit is optimised for the bulk assessment, only 85 out of 204 FT plumes are placed correctly. Apart from that, 50 ABL plumes are erroneously marked as the FT ones.

To improve the detection of the FT fires, a third fitting exercise was performed with the modified quality criterion:

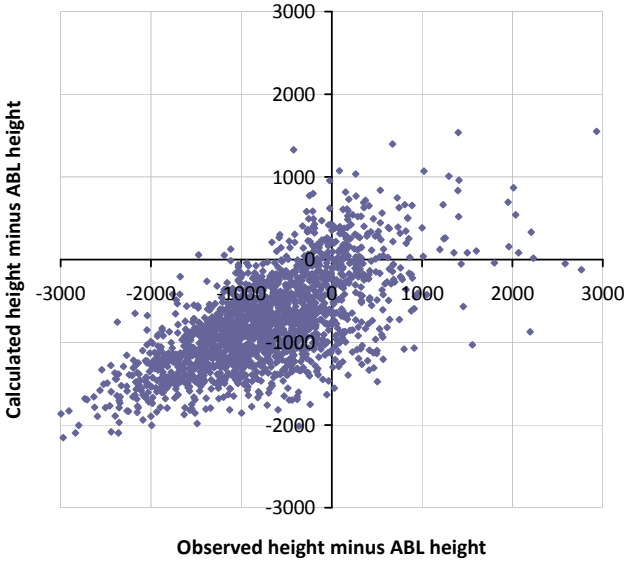

Fig. 5. Comparison of difference between the H_{abl} and the predicted (Eqs. 10, 13) and observed fire plume heights.

$$J_R = \sum_{i=1}^{N_{fires}} \Theta(-\Delta H_{obs}) \cdot \Theta(\Delta H_{mdl}) - 1.2 \sum_{i=1}^{N_{fires}} \Theta(\Delta H_{obs}) \cdot \Theta(\Delta H_{mdl}) \quad (20)$$

Here $\Delta H_{obs} = H_p^{obs}(i) - H_{ABL}(i)$, $\Delta H_{mdl} = H_p^{mdl}(i) - H_{ABL}(i)$. Minimisation of this function corresponds to the minimum fraction of the ABL-plumes misinterpreted as FT-ones (the first term) and the maximum fraction of the

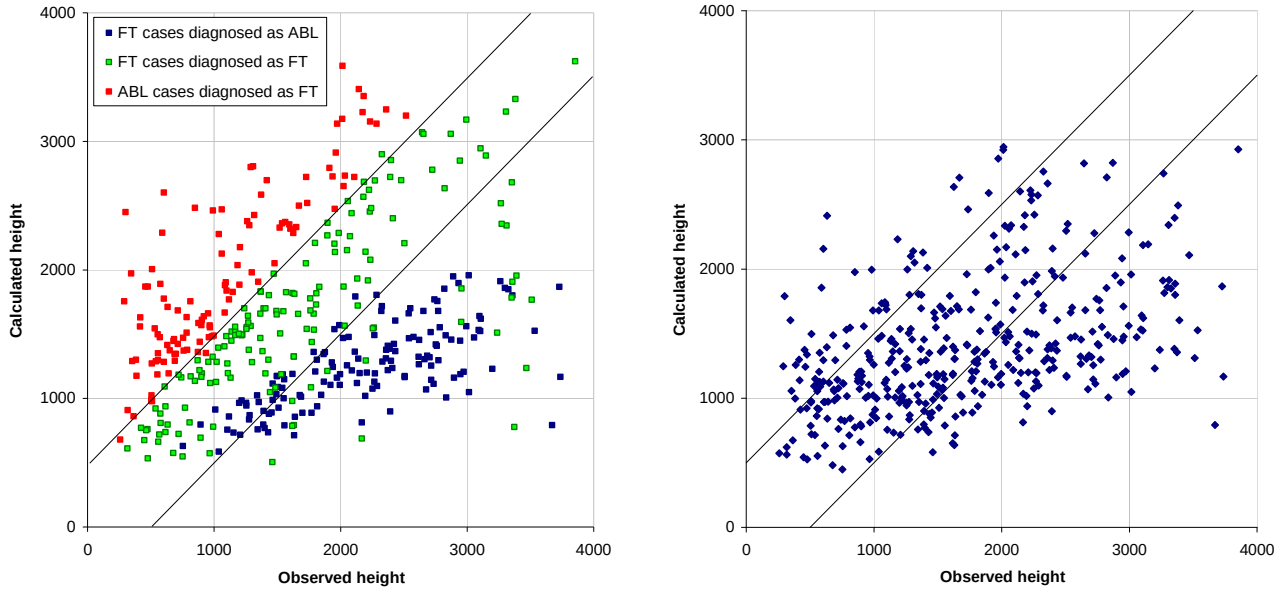

(a) Prediction with selection of ABL-FT cases (b) Prediction with the generic formula (10) and parameters (Eq. 13)

Fig. 6. Performance of the formulas (10, 19) for the cases detected as FT with the selection parameters (Eq. 21) (left-hand panel) and the general fit (Eq. 13) (right-hand panel).

FT-plumes recognised correctly (the second term). The scaling of 1.2 sets the priority to correct recognition of the FT cases over the misinterpretation of the ones inside the ABL.

The optimization with the cost function (Eq. 20) results in the following parameter values:

$$\alpha = 0.15\,; \quad \beta = 102\,\mathrm{m}\,; \quad \gamma = 0.49\,; \quad \delta = 0 \qquad (21)$$

It is seen that for accurate positioning of the plume regarding the ABL height, the FT stratification is unimportant, whereas the FRP is taken to power of 1/2, which is much larger than in all other fits.

Detection skills of this fit are better than those of the generic one: 110 out of 204 FT plumes are recognised correctly, with the rate of mis-located ABL plumes still being small: 70 out of ∼1000.

As a result, the following two-step procedure can be considered:

1. The injection height is evaluated using the formula (10) with parameters (Eq. 21).

2. The result is compared to H_{ABL} and, depending on $H_{\mathrm{p}} < H_{\mathrm{abl}}$, or $H_{\mathrm{p}} > H_{\mathrm{abl}}$, the final height is evaluated using the parameters (Eqs. 13 or 19), respectively.

Application of this procedure to the whole MISR set leads to slightly lower but still similar quality scores as the single-step computations: ∼64 % of the plumes are predicted within 500 m of the observations. This is not surprising because the bulk of the dataset are the ABL cases where little has changed.

For the FT plumes, however, the situation changes. As seen from Fig. 6a, the plumes observed and/or detected as the FT ones, fall to three clearly distinguishable groups: (i) the FT-plumes, which are correctly treated with FT-specific fit (Eq. 19) and predicted well (green dots in Fig. 6a), (ii) FT-plumes, which are wrongly treated with the ABL fit (Eq. 13) and under-estimated (blue dots); (iii) the ABL-plumes, which are erroneously treated with the FT fit (Eq. 19) and over-estimated (red dots).

The trade-off between the one-step and two-step estimations becomes clear from the comparison of the panels in Fig. 6. They both show the predictions for the same subset of fires but panel b shows the outcome of the single-step procedure using the generic coefficient (Eq. 13). As one can see, single-step predictions are practically free from the over-estimated cases but the fraction of the under-estimated plumes is large. However, the formal quality criteria (RMS, fraction of good predictions, etc.) are better for the one-step procedure. Therefore, the choice between the one-step and two-step approaches would depend on goals of the specific application.

Another peculiarity of the methodology, which would affect its application, is that the FRP is used as the only input information about the fire. We are not aware about any variable, which could replace FRP in the formulations (Eq. 10) and which would be as easily available from remote-sensing instruments as FRP. It can be related to the temperature anomaly following Sofiev et al. (2009) but the accuracy of that relation depends on the fire intensity and may be insufficient for small fires. Relations of FRP and sensible and latent

heat fluxes assumed for the simplified derivations (Eqs. 3–8) were used only to obtain a general form of the dependence and cannot be used for "reverse engineering" of FRP. Possibilities of using these or other proxy variables instead of FRP are outside this study.

7 Conclusions

The suggested methodology (Eq. 10) with parameters (Eqs. 13, 19) and the selection fit (Eq. 21) are based on three input parameters: boundary layer height, fire radiative power, and Brunt-Väisälä frequency in the FT.

The inside-ABL injection heights are predicted within the uncertainty range of the MISR observations (500 m) for about two thirds of the cases if all MISR data are considered and for >70 % of the cases if only "good" MISR data are taken. The existing parameterizations show much lower scores if a similar level of complexity of the approach is considered (e.g. Briggs formulas). Comparable, but still lower, scores were demonstrated only by the 1-D plume rise model – but with much greater input information and computational demands.

The FT-plumes comprise about 15 % of all cases and thus have a low impact upon the optimal parameters if all fires are considered. However, the fraction of well-predicted plume heights exceeds 80 % if the free-troposphere plumes are preselected.

The formula with parameters adapted for detection of the FT cases, is capable of catching about 60 % of the free-troposphere plumes; but it also mis-detects a few ABL plumes as belonging to the FT. Until this detection procedure is improved, selection of the single-formula approach or the two-step computations should be performed on a case-by-case basis.

Acknowledgements. The work has been done within the scope of TEKES-KASTU-2 and Academy of Finland IS4FIRES and ASTREX projects. Support of FP7-MACC, PASODOBLE and PEGASOS projects is kindly acknowledged. Discussions with E. Genikhovich and three anonymous reviewers are greatly appreciated.

Edited by: S. Kloster

References

Barry, R. G. and Chorley, R. J.: Atmosphere, weather and climate, 7th edn., 1998.

Berlyand, M. E.: Modern problems of admosheric diffusion and atmospheric pollution, Gidrometizdat, Leningrad, 1975 (in Russian).

Briggs, G. A.: Plume Rise, in: US Atomic Energy Commission Critical Review Series T/D 25075, US Atomic Energy Commission, Germantown, Maryland, p. 81, 1969.

Briggs, G. A.: Plume rise predictions, in: Lectures on air pollution and environmental impact analyses, Boston, 59–111, 1975.

Briggs, G. A.: Plume rise and buoyancy effects, in: Atmospheric science and power production, edited by: Anderson, D., US Department of Energy, Germantown, Maryland, p. 855, 1984.

Brown, D. F.: An Improved Methodology for Characterizing Atmospheric Boundary Layer, Turbulence and Dispersion, Ph.D. thesis, University of Illinois, Urbana, 150 pp., 1997.

Brown, D. F., Dunn, W. E., Policastro, A. J., and Maloney, D.: FIREPLUME Model for Plume Dispersion from Fires: Application to Uranium Hexafluoride Cylinder Fires, Illinois, available at: http://www.osti.gov/bridge/servlets/purl/510554-2x6vjV/webviewable/510554.pdf, 1997.

Davison, P. S.: Estimating the direct radiative forcing due to haze from the 1997 forest fires in Indonesia, J. Geophys. Res., 109, 1–12, doi:10.1029/2003JD004264, 2004.

Dozier, J.: A method for satellite identification of surface temperature fields of subpixel resolution, Remote Sens. Environ., 11, 221–229, doi:10.1016/0034-4257(81)90021-3, 1981.

Forster, C., Wandinger, U., Wotawa, G., James, P., Mattis, I., Althausen, D., Simmonds, P., O'Doherty, S., Jennings, S. G., Kleefeld, C., Schneider, J., Trickl, T., Kreipl, S., Jäger, H., and Stohl, A.: Transport of boreal forest fire emissions from Canada to Europe, J. Geophys. Res., 106, 22887–22906, doi:10.1029/2001JD900115, 2001.

Freitas, S. R., Longo, K. M., Chatfield, R., Latham, D., Silva Dias, M. A. F., Andreae, M. O., Prins, E., Santos, J. C., Gielow, R., and Carvalho Jr., J. A.: Including the sub-grid scale plume rise of vegetation fires in low resolution atmospheric transport models, Atmos. Chem. Phys., 7, 3385–3398, doi:10.5194/acp-7-3385-2007, 2007.

Freitas, S. R., Longo, K. M., Trentmann, J., and Latham, D.: Technical Note: Sensitivity of 1-D smoke plume rise models to the inclusion of environmental wind drag, Atmos. Chem. Phys., 10, 585–594, doi:10.5194/acp-10-585-2010, 2010.

Fromm, M., Jerome, A., Hoppel, K., Hornstein, J., Bevilacqua, R., Shettle, E., Servranckx, R., Zhanqing, L., and Stocks, B.: Observations of boreal forest fire smoke in the stratosphere by POAM III, SAGE II, and lidar in 1998, Geophys. Res. Lett., 27, 1407–1410, doi:10.1029/1999GL011200, 2000.

Gostintsev, Y. A., Kopylov, N. P., Ryzhov, A. M., and Khazanov, I. R.: Numerical modelling of convective flows above large fires at various atmopsheric conditions, Fizika goreniya i vzryva, 27, 10–17, 1991.

Guldberg, P. H.: A comparison study of plume rise formulas applied to tall stack data, J. Appl. Meteor. Climatol., 14, 1402–1405, 1975.

Huber, P. J.: Robust statistics, John Wiley and Sons, Hoboken, New Jersey, 1981.

Kahn, R. A., Li, W.-H., Moroney, C., Diner, D. J., Martonchik, J. V., and Fishbein, E.: Aerosol source plume physical characteristics from space-based multiangle imaging, J. Geophys. Res., 112, 1–20, doi:10.1029/2006JD007647, 2007.

Kahn, R. A., Chen, Y., Nelson, D. L., Leung, F.-Y., Li, Q., Diner, D. J., and Logan, J. A.: Wildfire smoke injection heights: Two perspectives from space, Geophys. Res. Lett., 35, 4–7, doi:10.1029/2007GL032165, 2008.

Kaufman, I., Steele, M., Cummings, D. L., and Jaramillo, V. J.: Biomass dynamics associated with deforestation, fire, and, conversion to cattle pasture in a Mexican tropical dry forest, Forest Ecol. Manag., 176, 1–12, 2003.

Kaufman, Y. J., Justice, C. O., Flynn, L. P., Kendall, J. D., Prins, E. M., Giglio, L., Ward, D. E., Menzel, W. P., and Setzer, A. W.: Potential global fire monitoring from EOS-MODIS, J. Geophys. Res.-Atmos., 103, 32215–21238, 1998.

Labonne, M., Bréon, F.-M., and Chevallier, F.: Injection height of biomass burning aerosols as seen from a spaceborne lidar, Geophys. Res. Lett., 34, 1–5, doi:10.1029/2007GL029311, 2007.

Lavdas, L. G.: Program VSMOKE – Users Manual, Gen. Tech. Rep. SRS-6, 1996.

Lavoué, D., Liousse, C., Cachier, H., Stocks, B. J., and Goldammer, J. G.: Modeling of carbonaceous particles emitted by boreal and temperate wildfires at northern latitudes, J. Geophys. Res., 105, 26871–26890, doi:10.1029/2000JD900180, 2000.

Lim, A., Liew, S. C., Lim, K. H., and Kwoh, L. K.: Computation of subpixel fire temperature with MODIS data, in: 22nd Asian Conference on Remote Sensing, Asian Association of Remote Sensing, Singapore, 2001.

Liousse, C., Penner, J. E., Chuang, C., Walton, J. J., Eddleman, H., and Cachier, H.: A global three-dimensional model study of carbonaceous aerosols, J. Geophys. Res., 101, 19411–19432, doi:10.1029/95JD03426, 1996.

Liu, Y., Achtemeier, G. L., Goodrick, S. L., and Jackson, W. A.: Important parameters for smoke plume rise simulation with Daysmoke, Atmospheric Pollution Research, 1, 250–259, 2010.

Luderer, G., Trentmann, J., Winterrath, T., Textor, C., Herzog, M., Graf, H. F., and Andreae, M. O.: Modeling of biomass smoke injection into the lower stratosphere by a large forest fire (Part II): sensitivity studies, Atmos. Chem. Phys., 6, 5261–5277, doi:10.5194/acp-6-5261-2006, 2006.

Martin, D., Webber, D. M., Jones, S. J., Underwood, B. Y., Tickle, G. A., and Ramsdale, S. A.: Near- and intermediate-field dispersion from strongly buoyant sources, AEAT/1388, Final Report, 1997.

Mazzoni, D., Logan, J. A., Diner, D., Kahn, R. A., Tong, L., and Li, Q.: A data-mining approach to associating MISR smoke plume heights with MODIS fire measurements, Remote Sens. Environ., 107, 138–148, 2007.

Moncrieff, M. W. and Miller, M. J.: The dynamics and simulation of tropical cumulonimbus and squall lines, Q. J. Roy. Meteorol. Soc., 102, 373–394, doi:10.1002/qj.49710243208, 1976.

Nikmo, J., Tuovinen, J.-P., Kukkonen, J., and Valkama, I.: A hybrid plume model for local-scale atmospheric dispersion, Atmos. Environ., 33, 4389–4399, doi:10.1016/S1352-2310(99)00223-X, 1999.

Pfister, G. G., Avise, J., Wiedinmyer, C., Edwards, D. P., Emmons, L. K., Diskin, G. D., Podolske, J., and Wisthaler, A.: CO source contribution analysis for California during ARCTAS-CARB, Atmos. Chem. Phys., 11, 7515–7532, doi:10.5194/acp-11-7515-2011, 2011.

Seinfeld, J. H. and Pandis, S. N.: Atmospheric chemistry and physics. From air pollution to climate change, 2nd edn., John Wiley & Sons, Inc., Hoboken, New Jersey, 2006.

Sofiev, M., Siljamo, P., Valkama, I., Ilvonen, M., and Kukkonen, J.: A dispersion modelling system SILAM and its evaluation against ETEX data, Atmos. Environ., 40, 674–685, doi:10.1016/j.atmosenv.2005.09.069, 2006.

Sofiev, M., Vankevich, R., Lotjonen, M., Prank, M., Petukhov, V., Ermakova, T., Koskinen, J., and Kukkonen, J.: An operational system for the assimilation of the satellite information on wildland fires for the needs of air quality modelling and forecasting, Atmos. Chem. Phys., 9, 6833–6847, doi:10.5194/acp-9-6833-2009, 2009.

Sukhinin, A. I., Conard, S. G., McRae, D. J., Ivanova, G. A., Tsvetkov, P. A., Bychkov, V. A., and Slinkina, O. A.: Remote Sensing of Fire Intensity and Burn Severity in Forests of Central Siberia, in: Contemporary Problems of Earth Remote Sensing from Space, Space Research Institute RAS., Mscow, available at: http://www.iki.rssi.ru/earth/ppt2005/sukhinin.pdf, 2005.

Trentmann, J., Luderer, G., Winterrath, T., Fromm, M. D., Servranckx, R., Textor, C., Herzog, M., Graf, H.-F., and Andreae, M. O.: Modeling of biomass smoke injection into the lower stratosphere by a large forest fire (Part I): reference simulation, Atmos. Chem. Phys., 6, 5247–5260, doi:10.5194/acp-6-5247-2006, 2006.

Val Martin, M., Logan, J. A., Kahn, R. A., Leung, F.-Y., Nelson, D. L., and Diner, D. J.: Smoke injection heights from fires in North America: analysis of 5 years of satellite observations, Atmos. Chem. Phys., 10, 1491–1510, doi:10.5194/acp-10-1491-2010, 2010.

Wang, J., Christopher, S. A., Nair, U. S., Reid, J. S., Prins, E. M., Szykman, J., and Hand, J. L.: Mesoscale modeling of Central American smoke transport to the United States: 1. "Top-down" assessment of emission strength and diurnal variation impacts, J. Geophys. Res., 111, 1–21, doi:10.1029/2005JD006416, 2006.

Weil, J.: Plume rise, in: Lectures on Air Pollution Modelling, edited by: Venkatram, A. and Wingaard, J. C., American Meteorological Soc., Boston, p. 390, 1988.

Westphal, L. and Toon, O. B.: Simulations of Microphysical, Radiative, and Dynamical Processes in a Continental-Scale Forest Fire Smoke Plume, J. Geophys. Res., 96, 22379–22400, doi:10.1029/91JD01956, 1991.

Zilitinkevich, S. S., Elperin, T., Kleeorin, N., and Rogachevskii, I.: Energy- and flux budget (EFB) turbulence closure model for stably stratified flows. Part I: Steady-state, homogeneous regimes, Bound.-Lay. Meteorol., 125, 167–192, 2007.